Supporting Information

A Double-Leg Donor-Acceptor Molecular Elevator: New Insight into Controlling the Distance of Two Platforms

Zhi-Jun Zhang,[a] Min Han,[a,b] Heng-Yi Zhang,[a] and Yu Liu *,[a]

[a] Department of Chemistry, State Key Laboratory of Elemento-Organic Chemistry, Nankai University, Tianjin 300071, P. R. China

[b] Traditional Chinese Medicine Research & Development Institute of Tasly Academy, Tianjin Tasly Group Co. Ltd., Tianjin 300410, P. R. China

yuliu@nankai.edu.cn

Table of Contents

General methods and materials: All chemicals were commercially available unless noted otherwise. All chemicals were commercially available unless noted otherwise. **1**[1], **2**-2H·2PF_6[2], **5**-2H·2PF_6[2], **6**-2H·4PF_6[2], and 3,5-di(*tert*-butyl)benzyl azide[3] were prepared according to the literature procedure. NMR data were recorded on Bruker AV400 spectrometer, and chemical shifts were recorded in parts per million (ppm). Mass spectra were recorded using Agilent 6520 Q-TOF LC/MS (ESI). Absorption spectra were recorded on Shimadzu UV/Vis spectrometer UV-2401PC. Fluorescence spectra were measured with an Edinburgh Analytical Instruments FLS920 spectrometer (Edinburgh Instruments, Edinburgh, U.K.) employing the time correlated single photon counting technique.

Preparation of **3**-2H·2PF_6:

2-2H·2PF_6 (81 mg, 0.08 mmol), **1** (100 mg, 0.10 mmol), 3,5-di(*tert*-butyl)benzyl azide (60 mg, 0.24 mmol), $Cu(MeCN)_4PF_6$ (112 mg, 0.30 mmol) and 2,6-lutidine (3.2 mg, 0.03 mmol) were mixed in 3 mL CH_3CN and 1 mL CH_2Cl_2, then stirred at room temperature for 24 h. After the solvent was reduced under vacuum, the residue was purified by column chromatography over silica gel (eluent: CH_2Cl_2/MeOH = 100:1) to afford the **3**-2H·2PF_6 as a dark green solid (104 mg, 53%). ^{1}H NMR (400 MHz, CD_3CN) δ 8.40 (s, 4H), 8.03 (s, 2H), 7.45 (m, 6H), 7.35 (s, 4H), 7.23 (d, J = 1.4 Hz, 4H), 7.02–6.87 (m, 16H), 5.56 (s, 4H), 5.12 (s, 4H), 4.82–4.68 (m, 4H), 4.62–4.47 (m, 4H), 4.30 (m, 4H), 4.16 (m, 4H), 4.1–3.86 (m, 28H), 3.80 (m, 4H), 3.71–3.59 (m, 8H), 3.55 (m, 4H), 2.85–2.75 (m, 4H), 2.17–2.13(m, 4H), 1.49–1.41 (m, 4H), 1.30 (s, 36H), 1.05 (t, J = 7.3 Hz, 6H). ^{13}C NMR (100 MHz, CD_3CN) δ 162.4, 158.8, 151.6, 147.4, 146.9, 143.5, 135.0, 130.5, 129.7, 128.7, 125.7, 125.3, 124.4, 123.9, 122.5, 121.5, 115.1, 112.9, 103.3, 70.6, 70.1, 68.4, 68.1, 67.8, 61.4, 54.1, 50.2, 45.7, 38.4, 34.5, 30.5, 24.5, 23.1, 22.2, 13.9. HRMS (ESI): m/z: $[M–2PF_6]^{2+}$ calcd for $C_{126}H_{158}N_{10}O_{22}^{2+}$ 1082.0787; found: 1082.0785.

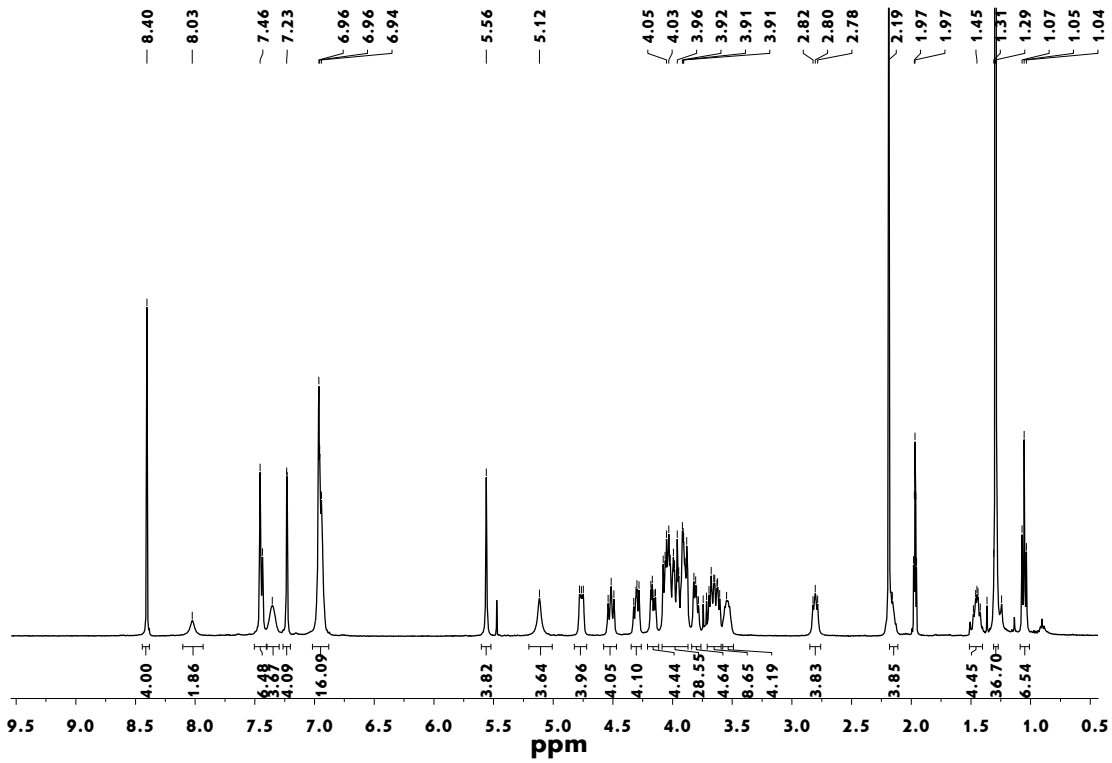

Figure S1. ^{1}H NMR spectrum of **3**-2H·2PF$_6$ (CD_3CN, 400 MHz, 298 K).

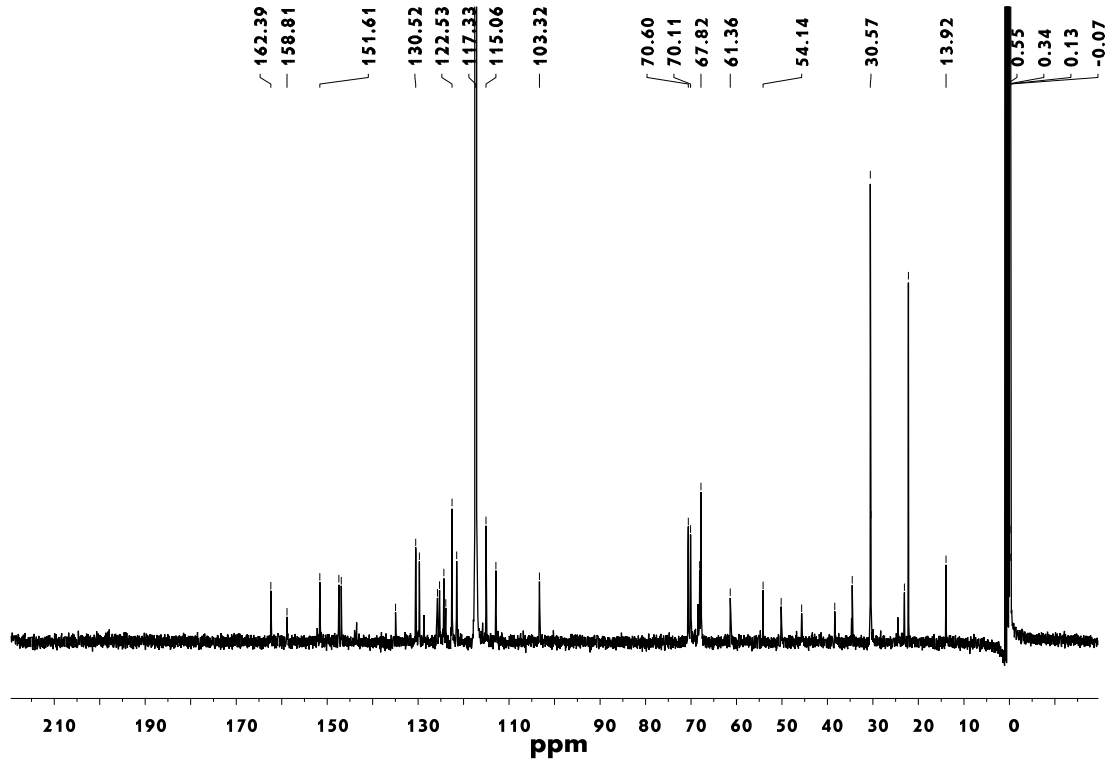

Figure S2. ^{13}C NMR spectrum of **3**-2H·2PF$_6$ (CD_3CN, 100 MHz, 298 K).

Preparation of **4**-2H·4PF_6:

To a solution of **3**-2H·2PF_6 (40 mg, 0.016 mmol) in 5 ml CH_3CN was added 5 ml CH_3I. The mixture was heated at 40 °C for 4 days. Then the solvent was removed under reduced pressure. When the crude product was suspended in acetone (40 ml), a saturated aqueous solution of NH_4PF_6 was added and the mixture stirred until the suspension became clear. The solvent was removed, and water (100 ml) was added to the residue. The resulting mixture was then filtered, washed with water, and dried to afford **4**-2H·4PF_6 as a pale green solid (32 mg, 72%). ^{1}H NMR (400 MHz, CD_3CN) δ 8.46 (s, 2H), 8.44 (s, 4H), 7.58 (s, 2H), 7.50 (d, J = 8.7 Hz, 4H), 7.41 (br, 4H), 7.38 (d, J = 1.4 Hz, 4H), 6.98 (s, 4H), 6.94 (m, 12H), 5.73 (s, 4H), 5.21 (s, 4H), 4.82 (m, 4H), 4.57–4.51 (m, 4H), 4.32 (m, 4H), 4.28 (m, 6H), 4.17–4.08 (m, 12H), 4.02 (m, 8H), 3.96–3.90 (m, 12H), 3.87–3.82 (m, 4H), 3.73–3.66 (m, 8H), 3.56 (m, 4H), 2.83 (m, 4H), 2.22 (m, 4H), 1.46 (m, 4H), 1.34 (s, 36H), 1.06 (t, J = 7.3 Hz, 6H). ^{13}C NMR (100 MHz, CD_3CN) δ 163.1, 158.2, 152.8, 148.0, 147.5, 140.4, 131.8, 131.3, 130.3, 129.8, 129.3, 127.4, 126.4, 126.0, 125.0, 124.5, 124.2, 122.1, 115.6, 113.5, 103.9, 71.3, 70.7, 68.7, 68.3, 58.7, 58.4, 50.5, 46.3, 39.2, 39.0, 35.3, 31.1, 25.0, 23.7, 14.5. HRMS (ESI): m/z: $[M–4PF_6]^{4+}$ calcd for $C_{128}H_{164}N_{10}O_{22}^{4+}$ 548.5508; found: 548.5515.

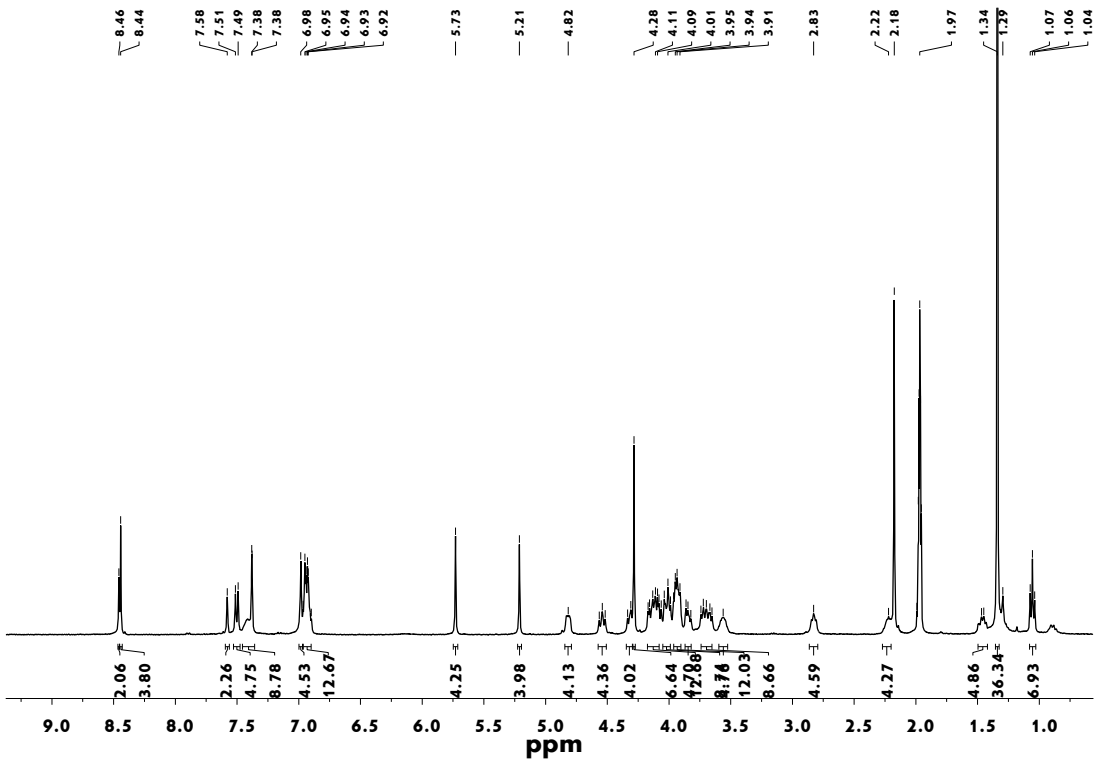

Figure S3. ^{1}H NMR spectrum of **4**-2H·4PF$_6$ (CD_3CN, 400 MHz, 298 K).

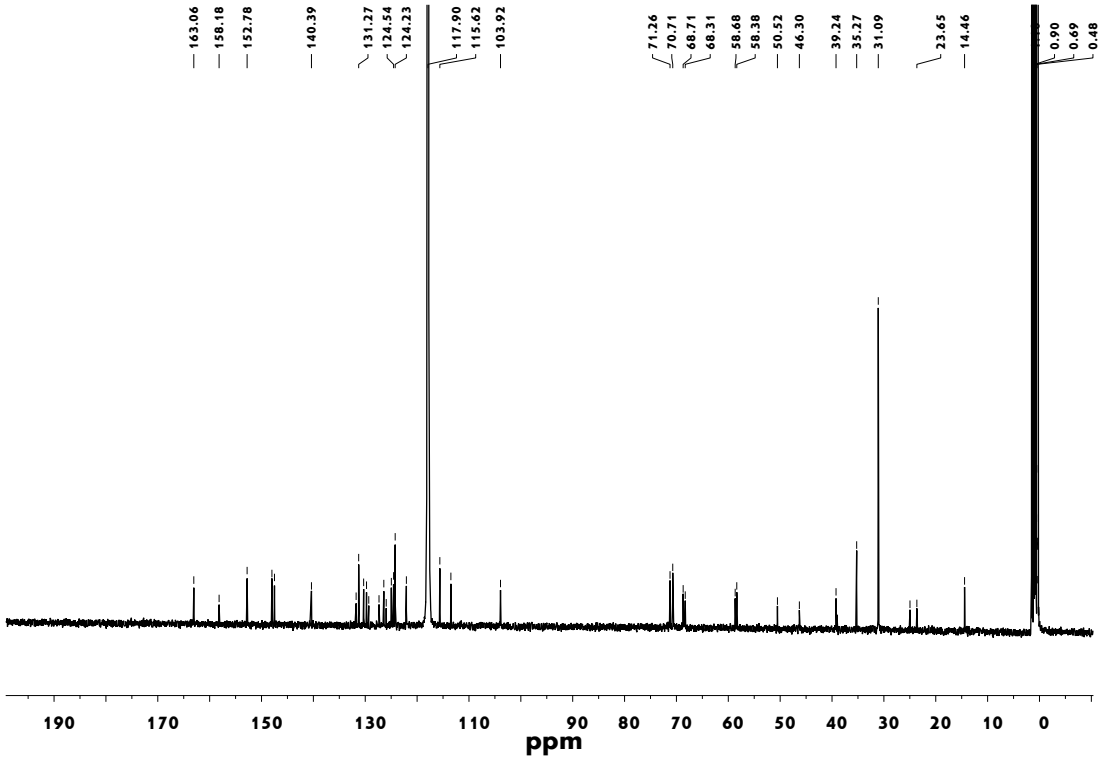

Figure S4. ^{13}C NMR spectrum of **4**-2H·4PF$_6$ (CD_3CN, 100 MHz, 298 K).

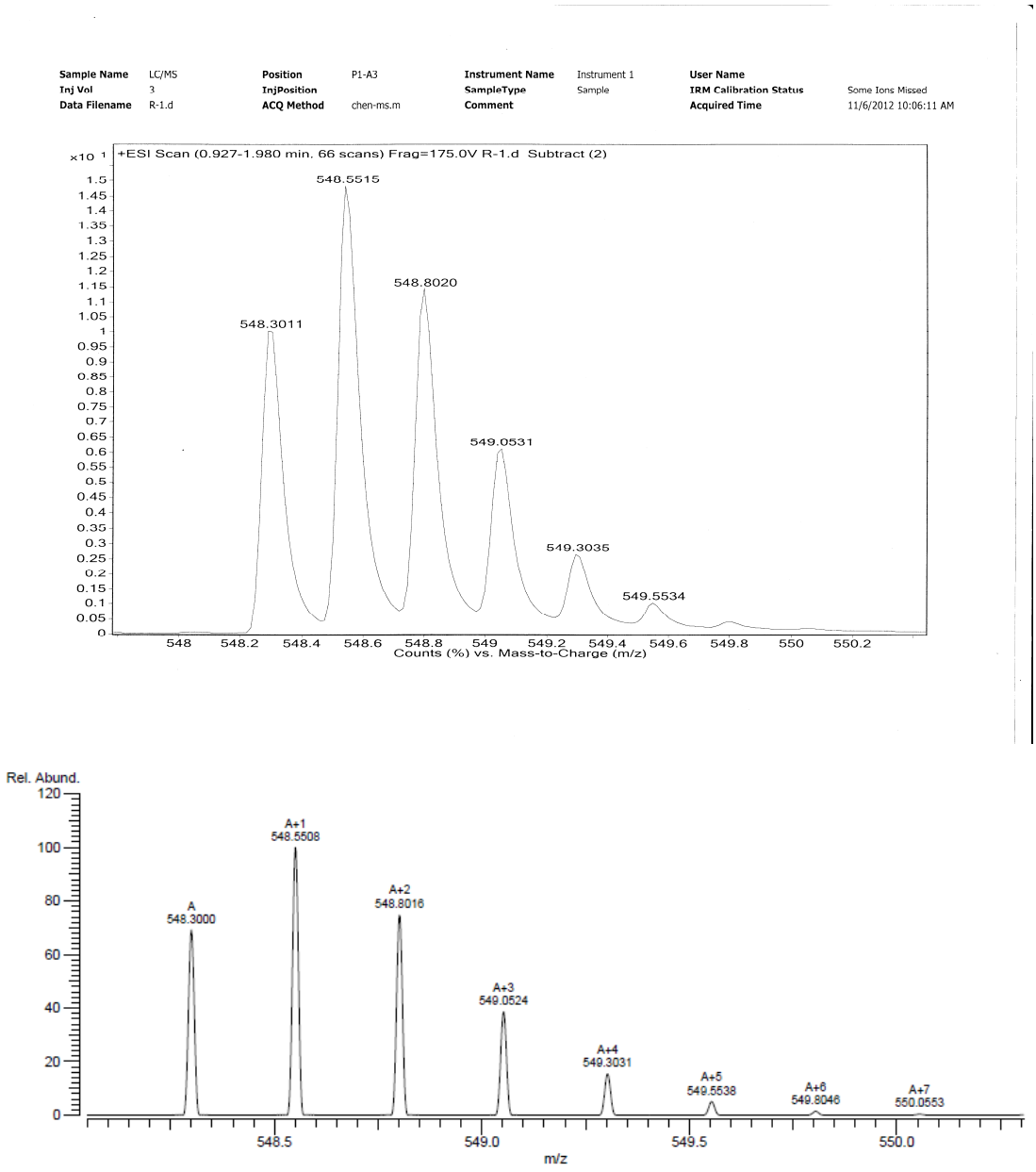

Figure S5. The HRMS spectrum of **4**-2H·4PF_6 (Top:experiment;bottom:calculation)

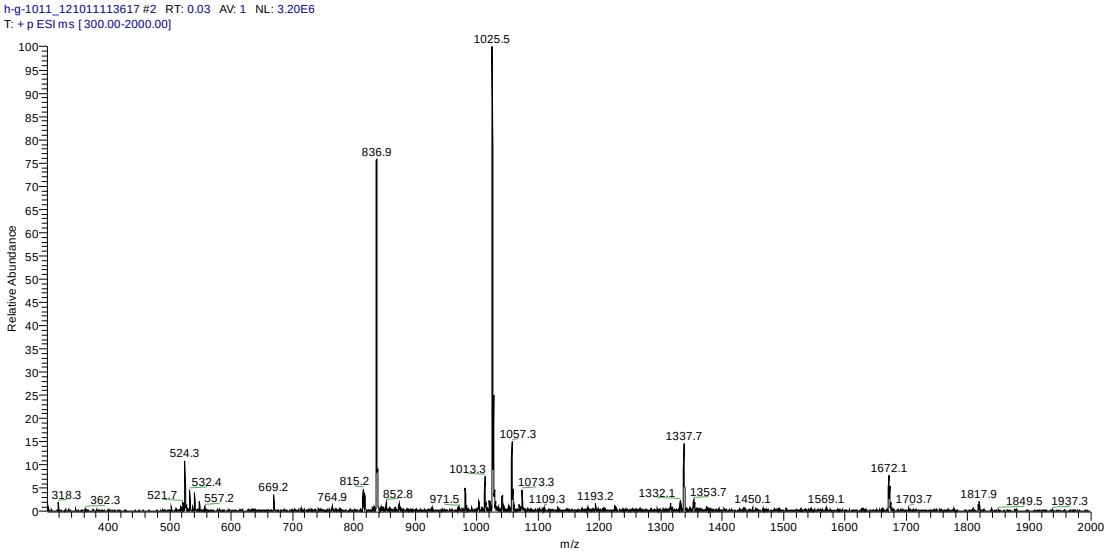

Figure S6. ESI-MS (low resolution) spectrum of the equimolar mixture of **1** and **2**-2H·2PF_6 in $CHCl_3$/CH_3CN (1:1). The major peak at m/z 837 is assigned to the dication [**1**·**2**-2H]$^{2+}$, the peak at m/z 1026 is assigned to [**1**+Na]$^{+}$

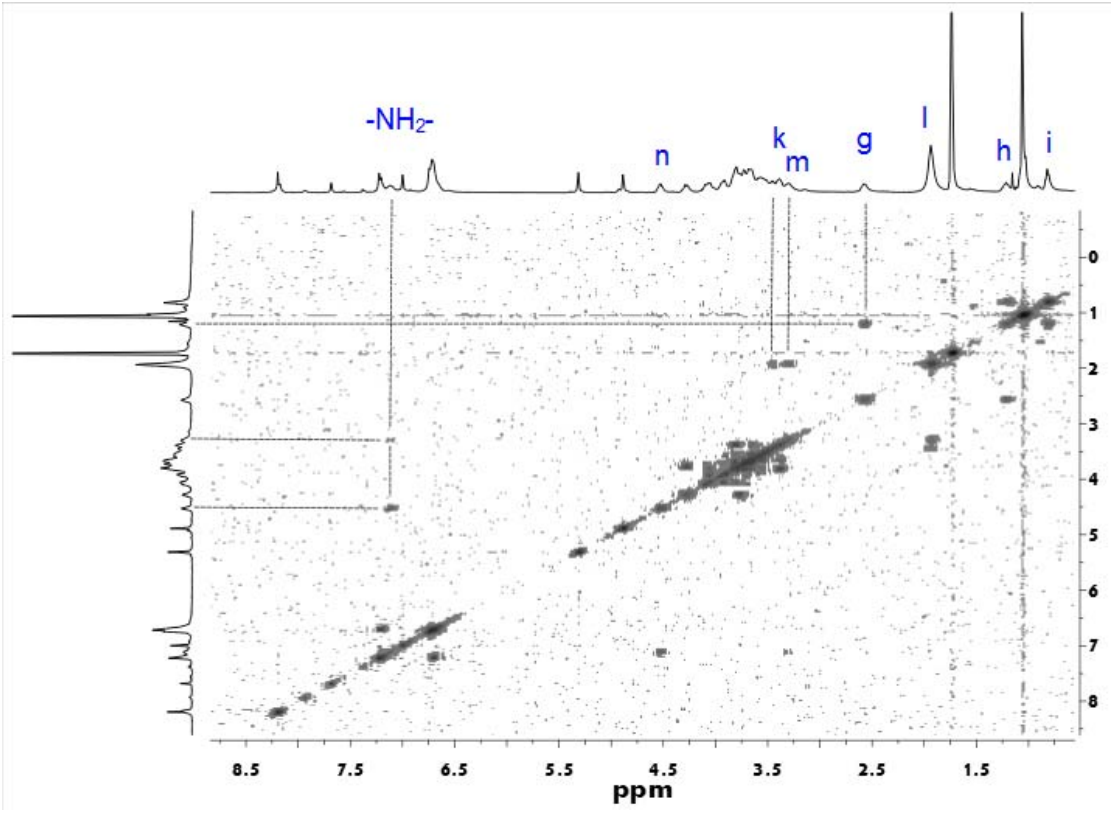

Figure S7. The ^{1}H-^{1}H COSY spectrum (400 MHz, 298 K, CD_3CN) of **3**-2H·2PF_6.

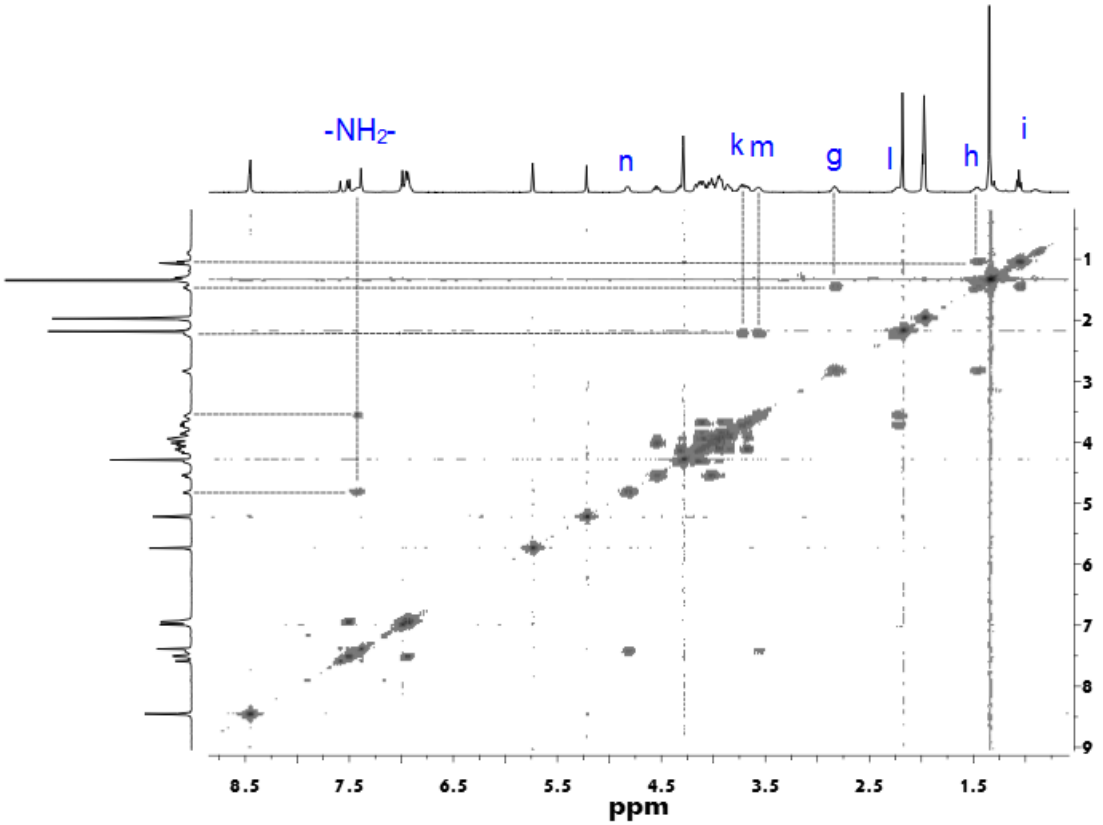

Figure S8. The ^{1}H-^{1}H COSY spectrum (400 MHz, 298 K, CD_3CN) of **4**-2H·4PF_6.

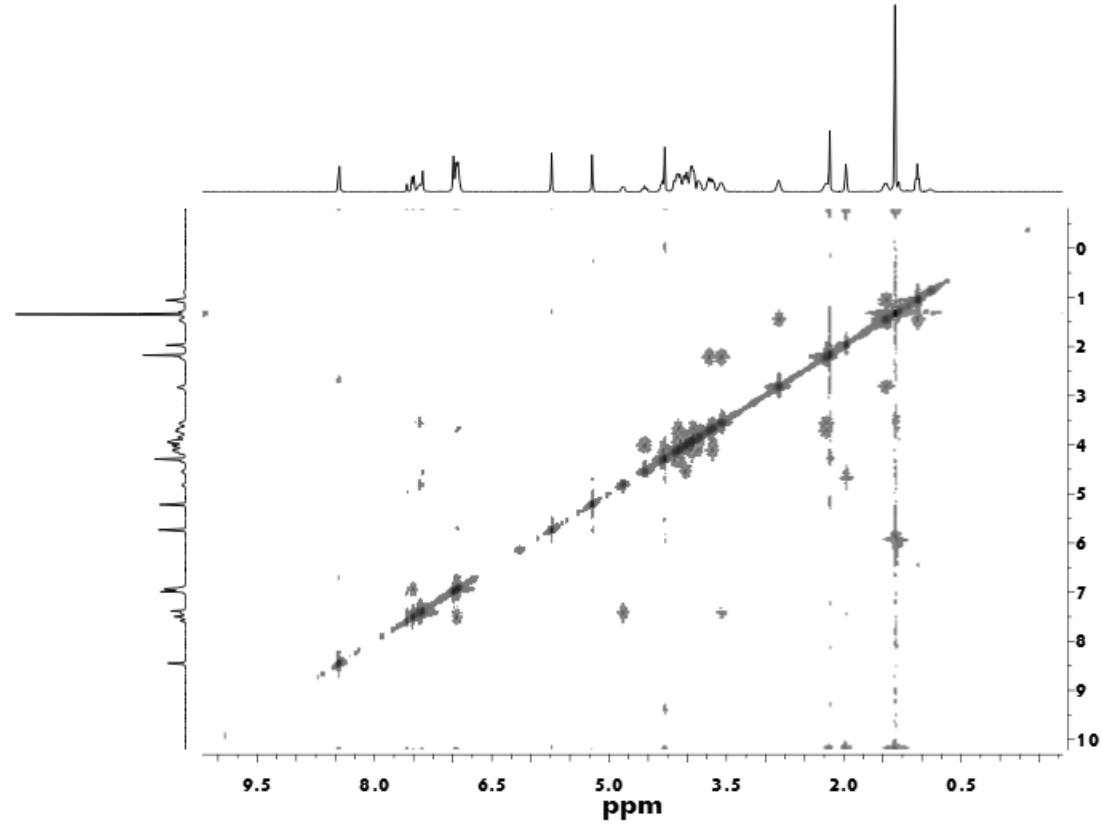

Figure S9. The NOESY spectrum (400 MHz, 298 K, CD_3CN) of **4**-2H·4PF_6.

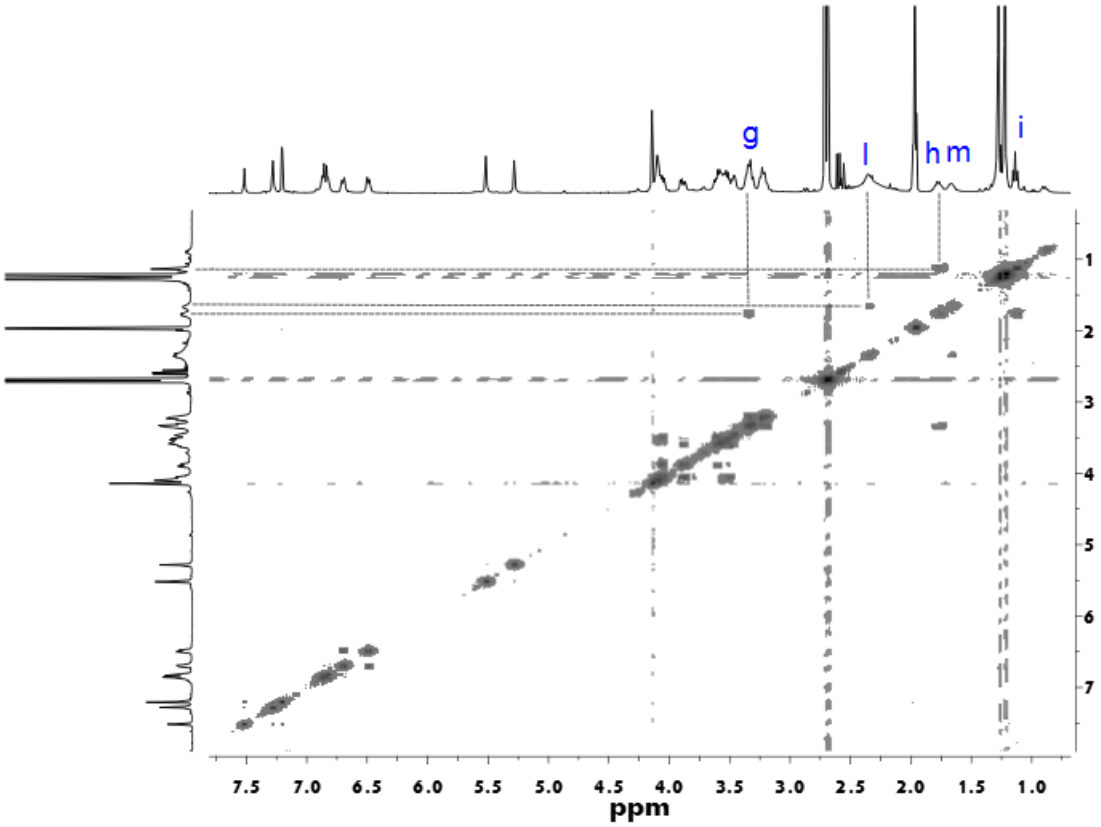

Figure S10. The ^{1}H-^{1}H COSY spectrum (400 MHz, 298 K, CD_3CN) of **4**-2H·4PF_6 after addition of 3.0 equivalents P_1–tBu.

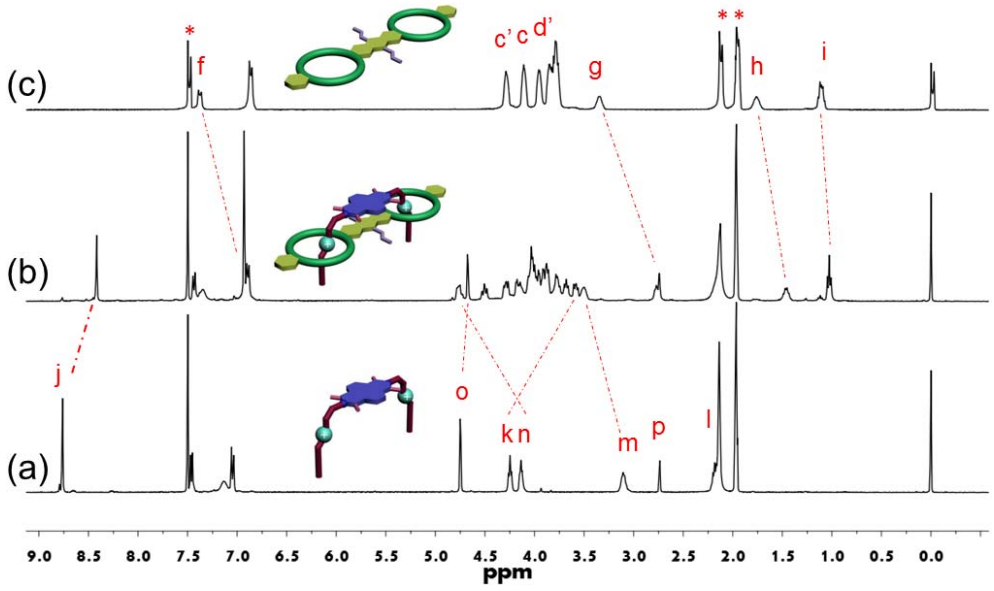

Figure S11. Partial ^{1}H NMR spectra (400 MHz, $CDCl_3/CD_3CN$ = 1:1, 5 mM, 298 K) of (a) **2**-2H·2PF_6, (b) 1:1 adduct [**1**·**2**-2H]·2PF_6, and (c) host **1**. * = peaks of solvents and H_2O.

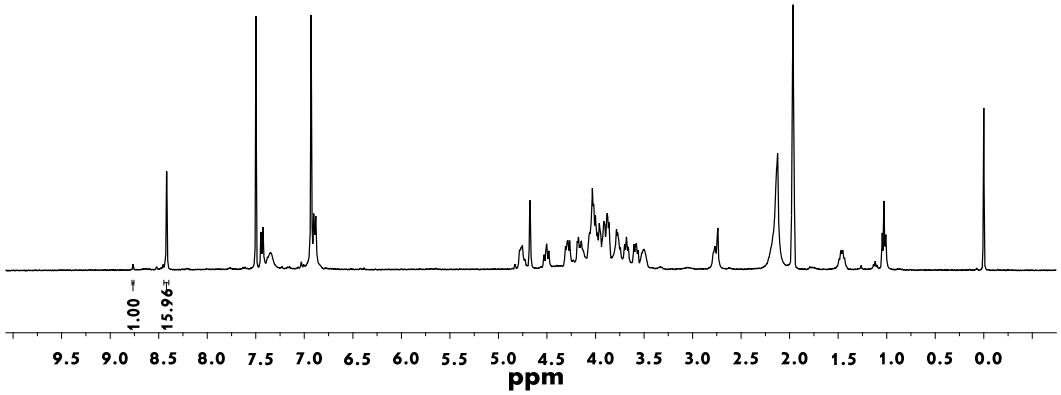

Figure S12. Partial ^{1}H NMR spectra (400 MHz, $CDCl_3/CD_3CN$ = 1:1, 5 mM, 298 K) of 1:1 adduct [**1**·**2**-2H]·2PF_6

The association constant of [**1**·**2**-2H]·2PF_6 was calculated by single-point method. From the integral ratio of complexed and uncomplexed H_j of **2**-2H·2PF_6, K_a = $[(15.96/16.96) \times 5.0 \times 10^{-3}] / [(1.0/16.96) \times 5.0 \times 10^{-3}]^2$ M^{-1} = 5.4×10^4 M^{-1}.

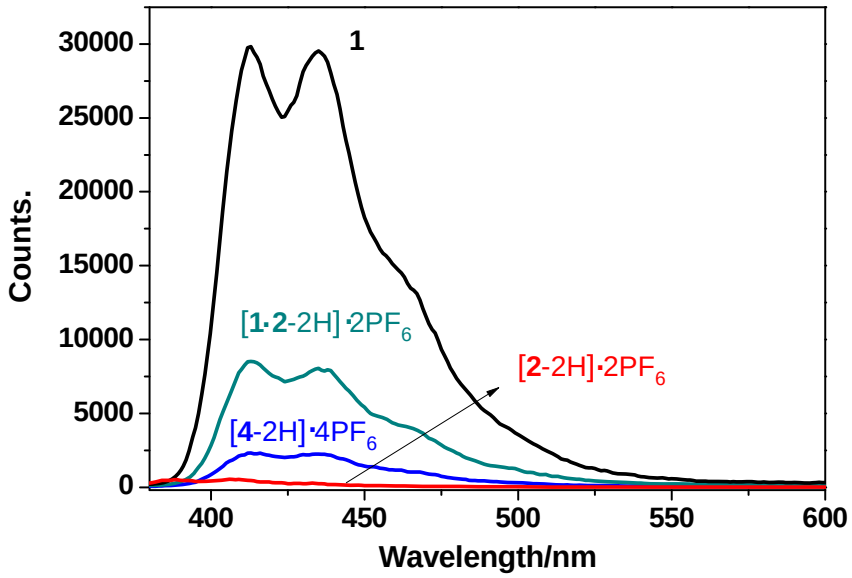

Figure S13. Emission spectra of a) **1**, b) **2**-2H·2PF_6, c) [**1**·**2**-2H]·2PF_6, and d) **4**-2H·4PF_6. ($CHCl_3/CH_3CN$ = 1:1, 0.01 mM, excited at λ = 375 nm)

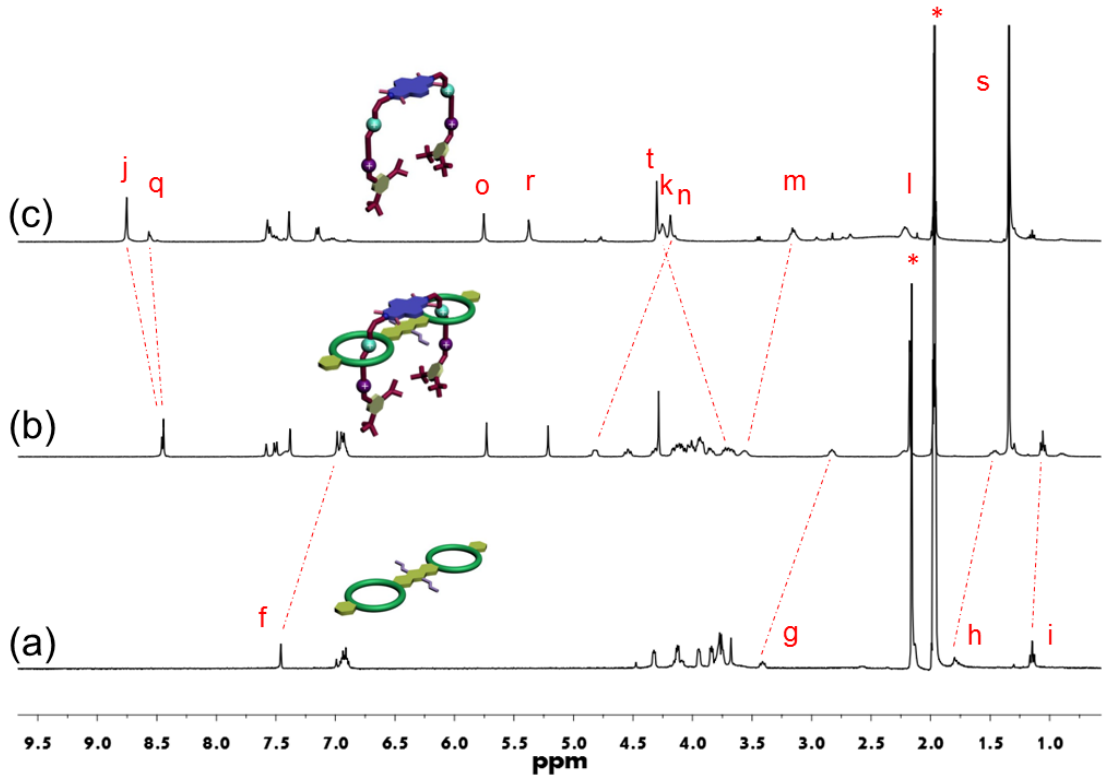

Figure S14. Partial ^{1}H NMR spectra (400 MHz, CD_3CN, 5 mM, 298 K) of (a) the uncomplexed host **1**, (b) **4**-2H·4PF_6, and (c) the uncomplexed dumbbell-shaped thread **6**-2H·4PF_6. * = peaks of solvent and H_2O.

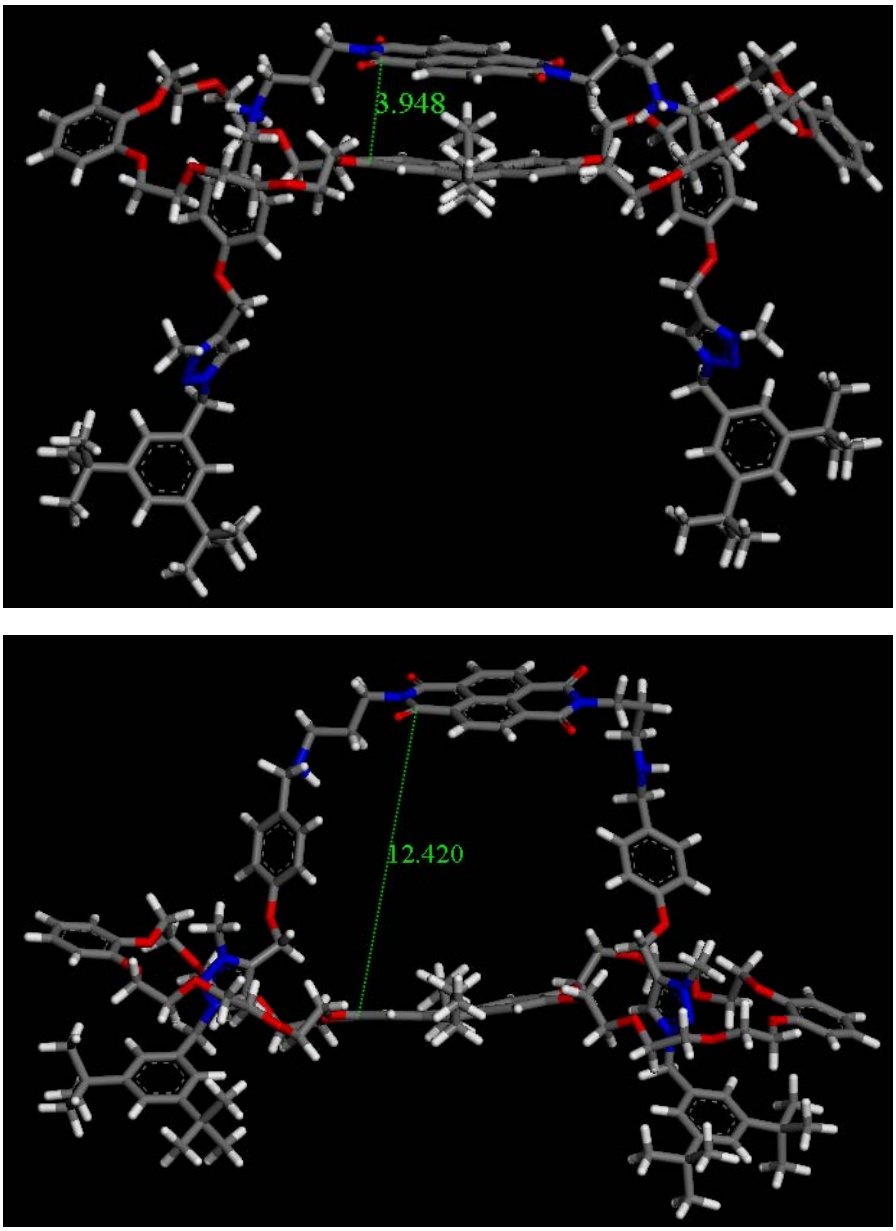

Figure S15. Molecular energy minimization of **4**-2H·4PF_6 with the platform situated on the upper level (top) and the lower level (bottom). The geometries were optimized by the molecular mechanics method with dreiding forcefield.

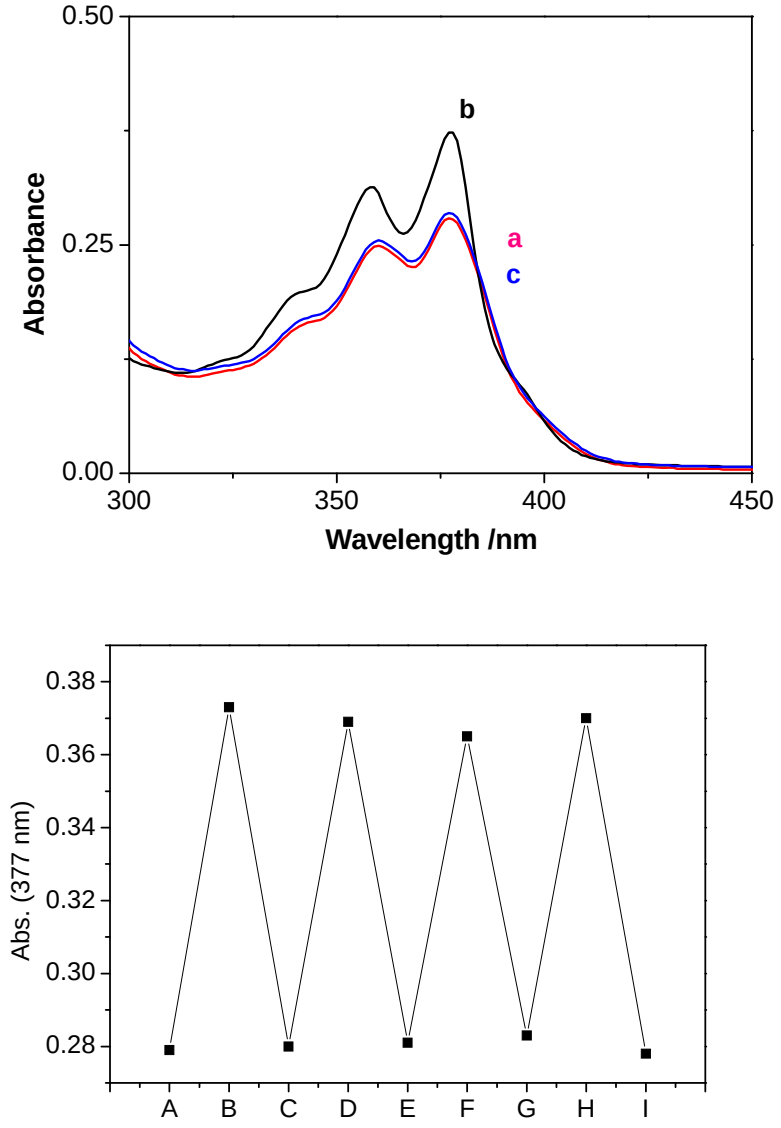

Figure S16. (Top) UV/vis spectra of a) **4**-2H·4PF_6, b) after the addition of 4.0 equiv of P_1–tBu to **4**-2H·4PF_6 and c) after the addition of 4.0 equiv of TFA to **4**-2H·4PF_6 treated by base. (CH_3CN, 0.01 mM)

(Bottom) Plot of absorption at 377 nm on successive addition of 4.0 equiv of P_1–tBu (B, D, F, H) and TFA (C, E, G, I).

In the dilute solution (0.01 mM), the spectral change can be only found below 450 nm, which should be attributed to the distance change of anthracene and NDI. After addition of base, the increase of absorption was consistent with the previous result on the divalent pseudorotaxane which also exhibits the similar change after addition of base Bu_3N.[1]

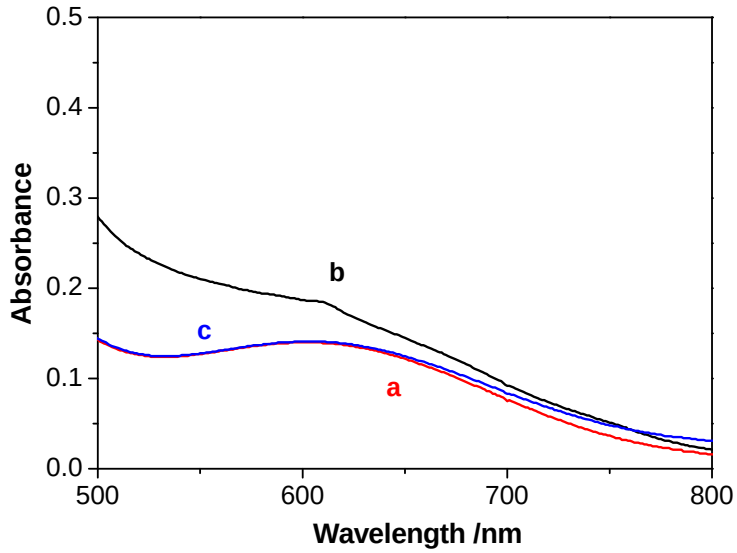

Figure S17. UV/vis spectra of a) **4**-2H·4PF_6, b) after the addition of 3.0 equiv of P_1–tBu to **4**-2H·4PF_6 and c) after the addition of 3.0 equiv of TFA to **4**-2H·4PF_6 treated by base. (CH_3CN, 1.5 mM)

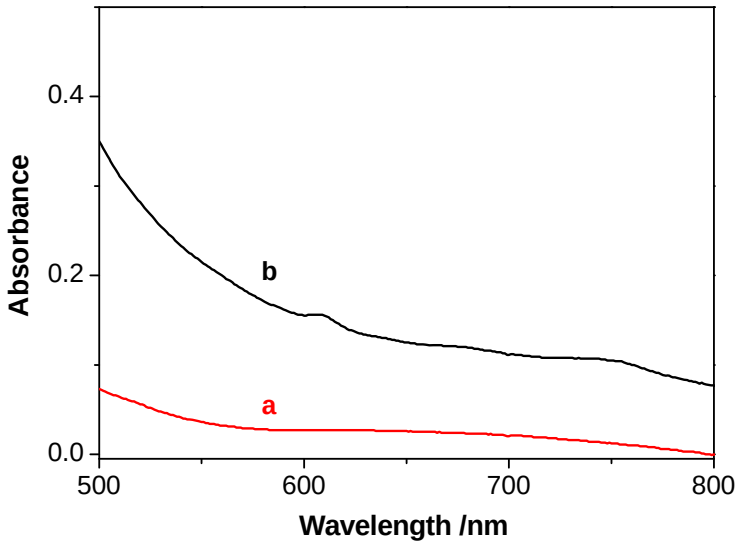

Figure S18. UV/vis spectra of a) **6**-2H·4PF_6, and b) after the addition of 3.0 equiv of P_1–tBu to **6**-2H·4PF_6. (CH_3CN, 1.5 mM).

After the addition of excessive base to the uncomplexed axle molecule **6**-2H·4PF_6, a strong CT absorption can be observed. It is noteworthy that a peak at 610 nm can be found which should be attributed to the anion radical state of NDI unit.[4] And this peak can be also found in the absorption spectrum of **4**-2H·4PF_6 after the addition of base (Figure S17b), which suggests that the phosphazene base not only moves the

elevator but also forms complex with the NDI unit as an electron donor. Moreover, through comparing the spectral change of **4**-2H·4PF_6 and **6**-2H·4PF_6 after addition of base, it can be suggested that after subtracting the CT interaction between P_1–tBu and NDI, the CT interaction between anthracene and NDI should be weakened.

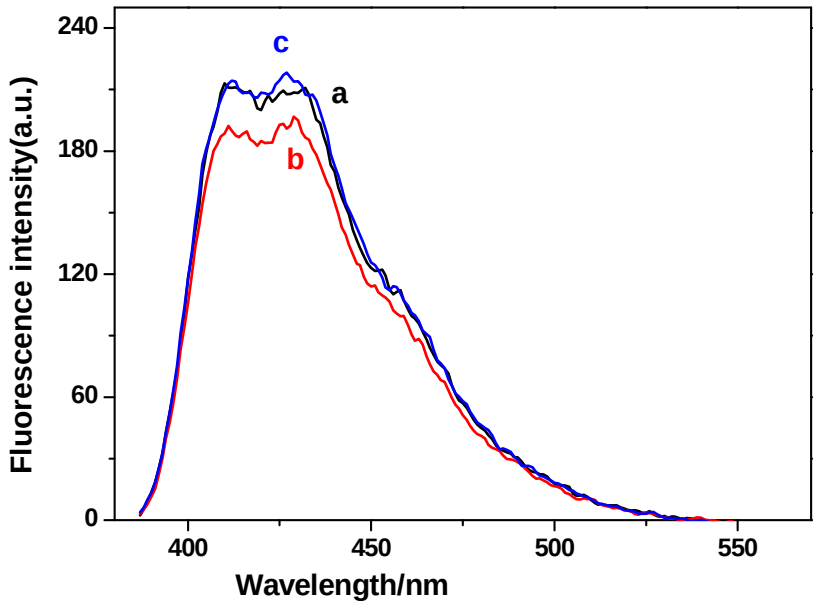

Figure S19. Emission spectra of a) **4**-2H·4PF_6, b) after the addition of 3.0 equiv of P_1–tBu to **4**-2H·4PF_6 and c) after the addition of 3.0 equiv of TFA to **4**-2H·4PF_6 treated by base. (CH_3CN, 0.01 mM, excited at λ = 375 nm)

References:

[1] Jiang, W.; Han, M.; Zhang, H. Y.; Zhang, Z. J.; Liu, Y. *Chem.–Eur. J.* **2009**, *15*, 9938–9945.

[2] Jiang, Q.; Zhang, H. Y.; Han, M.; Ding, Z. J.; Liu, Y. *Org. Lett.* **2010**, *12*, 1728–1731.

[3] Gassensmith, J. J.; Barr, L.; Baumes, J. M.; Paek, A.; Nguyen, A.; Smith, B. D. *Org. Lett.* **2008**, *10*, 3343–3346.

[4] Guha, S.; Saha, S. *J. Am. Chem. Soc.* **2010**, *132*, 17674–17677.